energies

MDPI

Review

Voltage Correction Factors for Air-Insulated Transmission Lines Operating in High-Altitude Regions to Limit Corona Activity: A Review

Jordi-Roger Riba [1,*], William Larzelere [2] and Johannes Rickmann [3]

[1] Electrical Engineering Department, Universitat Politècnica de Catalunya, 08220 Terrassa, Spain
[2] Evergreen High Voltage NY, PO Box 1758, Bolton Landing, NY 12814, USA; wel@ehvtest.com
[3] Siemens AG, Energy Management Division, Freyeslebenstr. 1, 91058 Erlangen, Germany; rickmann.johannes@siemens.com
* Correspondence: riba@ee.upc.edu; Tel.: +34-937-398-365

Received: 30 June 2018; Accepted: 19 July 2018; Published: 21 July 2018

Abstract: Nowadays there are several transmission lines projected to be operating in high-altitude regions. It is well known that the installation altitude has an impact on the dielectric behavior of air-insulated systems. As a result, atmospheric and voltage correction factors must be applied in air-insulated transmission systems operating in high-altitude conditions. This paper performs an exhaustive literature review, including state-of-the-art research papers and International Standards of the available correction factors to limit corona activity and ensure proper performance when planning air-insulated transmission lines intended for high-altitude areas. It has been found that there are substantial differences among the various correction methods, differences that are more evident at higher altitudes. Most high-voltage standards were not conceived to test samples to be installed in high-altitude regions and, therefore, most high-voltage laboratories are not ready to face this issue, since more detailed information is required. It is proposed to conduct more research on this topic so that the atmospheric corrections and altitude correction factors found in the current International Standards can be updated and/or modified so that high-voltage components to be installed in high-altitude regions can be tested with more accuracy, taking into account their insulation structure.

Keywords: high-voltage techniques; corona; critical disruptive voltage; high-altitude; correction factors

1. Introduction

When designing high-voltage electrical systems intended to be located at altitudes exceeding 1000 m it is imperative to know the effects of the atmospheric conditions on the specific components, otherwise it may result in premature aging, reduction of operation performance or even failure [1]. It is well known that the dielectric strength of air-insulated systems depends upon on the insulation structure, atmospheric conditions like temperature, pressure and humidity [2–4], as well as other factors such as the polarity and nature of the voltage applied [5]. The dielectric strength and transient overvoltage withstand levels are critical factors to design external insulation in power transmission systems [6]. In particular, high altitude decreases the air density which in turn lowers the dielectric withstand voltage for a given geometry and the overload capacity or thermal ampacity rating among others [7]. Effects such as pollution or icing occurring in high-altitude areas also lowers the dielectric performance of air-insulated systems [8]. Therefore, it is of paramount importance to know the critical disruptive voltage and corona inception voltage of the high-voltage components involved [9–11] for these specific conditions. It is known that for air at standard pressure, the inception voltage gradient is often above 15 kV_{peak}/cm [9] although values in the range from 6–30 kV_{peak}/cm can be found

depending on the geometry, gap length and polarity [12]. These values tend to be reduced when the air pressure is lower, as would be expected. Therefore, when dealing at standard pressure with conductors intended for overhead transmission lines with rated voltage above 110 kV, the surface voltage gradient is often limited to less than 16 kV_{RMS}/cm [13–15].

Extra-high voltage (EHV) and ultra-high voltage (UHV) power lines are the required means for transmitting large amounts of power over very long distances. However, due to the high voltage levels corona effects are increased [16,17]. Different high-altitude high-voltage tests were conducted in the United States during the 1950s and 1960s [18–20] driven by the need to construct transmission lines crossing high-altitude regions. Countries like China [21–25], India, Buthan [26], Nepal [27] and Peru [28], among others, have constructed or are proposing EHV transmission lines and the associated substations, crossing high-altitude regions. For example, the planned 500 kV Mantaro-Marcona-Socabaya-Montalvo transmission line in Peru will reach altitudes of about 4500 m above sea level and the Qinghai-Tibet transmission line in China crosses high-altitude regions with an average elevation of 4700 m and a maximum elevation of 5300 m. These projects face enormous technological challenges due to the severe atmospheric conditions existing in such regions.

The different International Standards reviewed in this paper suggest to apply voltage correction factors when operating in high-altitude areas or under non-standard atmospheric conditions, although they often give different indications [29]. In the technical literature there is a dispersion of results regarding voltage correction factors to be applied in high-voltage applications, whereas there is a lack of works reviewing and comparing such results, so this paper contributes in this area. It is worth noting that most of the high-voltage standards have not been conceived to deal with the problems that arise when the high-voltage devices to be tested must be installed in high-altitude regions, and most of the high-voltage laboratories are not prepared to face this problem due to the lack of contrasted information. This paper reviews the state-of-the-art of the available correction factors to limit corona activity and ensuring proper performance when planning air-insulated transmission lines intended for high-altitude areas. The paper provides a comprehensive review and a comparative analysis of the most popular atmospheric correction methods, including the latest research results, and analyzes their behavior to identify the weak points and challenges to be faced in order to update the International Standards involved.

2. Electric Field Formulas Based on Peek's Work

This section introduces the importance of the atmospheric conditions on the corona inception voltage and electric field. According to Peek [30–32] and Krasniqi et al. [33], when assuming two parallel and distant conductors, that is when they are far apart compared to their radius, the relationship between the line-to-neutral voltage U_{peak} (kV) and voltage gradient at the surface of the conductor E_{peak} (kV_{peak}/cm) is given by:

$$U_{peak} = E_{peak} r \ln(d/r) \tag{1}$$

where r is the radius of the conductor in cm and d the distance between conductors in cm for single-phase lines or the equivalent phase spacing for three-phase lines [34].

Since the atmospheric pressure has a strong impact on both corona inception [35] and disruptive discharge voltage, most of the relevant International Standards define normal service and HV (high voltage) testing altitude to be less than 1000 m [36–39]. The relative air density (RAD) δ is given by References [4,36,40]:

$$\delta = \frac{p}{p_0} \cdot \frac{273 + t_0}{t + 273} \tag{2}$$

It is worth noting that δ is unity at the standard reference atmosphere, that is, when the pressure of ambient air is $p = p_0 = 101.3$ kPa, its temperature is $t = t_0 = 20$ °C [36] and the absolute humidity is $h_a = 11$ g/m^3.

Despite the fact that Peek's work is a century old, its results are still used as a reference when designing transmission lines, so they are reviewed in this section. According to early work developed by Peek [30–32], the critical disruptive voltage that takes into account atmospheric conditions and the surface condition of the conductor can be written as:

$$U_{d,peak} = E_{d,peak} r m \delta \ln(d/r) \quad (3)$$

where $E_{d,peak}$ is the disruptive voltage gradient in kV_{peak}/cm, m the roughness factor of the conductor surface and δ the air density, which is defined in Equation (2). Therefore, from experimental results carried out with thin wires and a narrow interval of air density δ within 1.078–1.158 [18], Peek suggested that the critical disruptive voltage gradient E_d is almost proportional to the relative air density [41].

Typical values of the conductor surface roughness factor m based on weather conditions according to Cigré [41] are summarized in Table 1.

Table 1. Surface irregularity factor m [41].

Surface Irregularity Factor	Type of Surface
m = 1	Smooth and polished surface
m = 0.6–0.8	Dry weather
m = 0.3–0.6	Extreme pollution, snowflakes, raindrops
m = 0.25	Heavy rain

According to EPRI (Electric Power Research Institute) [14] and Westinghouse [34], common values of m for physical surface conditions are 0.84 for stranded conductors and 0.92 for segmental conductors.

Equation (3) assumes that for streamer discharges, the critical disruptive voltage at any atmospheric condition varies linearly with the air density δ. However, according to Westinghouse [34], the equation for critical disruptive voltage for parallel conductors is:

$$U_{d,phase-to-neutral,RMS} = E_{d,RMS} r m \delta^{2/3} \ln(d/r) \quad (4)$$

and therefore Equation (4) assumes that the critical disruptive voltage gradient $E_{d,RMS}$ in kV_{RMS}/cm is almost proportional to $\delta^{2/3}$, which is in contradiction with Peek's empirical formula, that was obtained from experiments with small radius thin wires and was carried out in a narrow range of relative air densities (RAD).

According to several authors [14,34,41–44] by applying Peek's law, the visual AC corona inception field strength in kV_{peak}/cm at power frequency for an isolated conductor or for two parallel conductors of radius r (cm) can be calculated from:

$$E_{c,peak} = E_{0,peak} m \delta (1 + 0.301/\sqrt{\delta r}) \quad (5)$$

where E_0 = 30 kV_{peak}/cm is the disruptive visual gradient [30] measured at 25 °C and 101.325 Pa [41]. Note that the visual corona inception voltage is lower than the critical disruptive voltage [30].

Peek's law for visual corona inception voltage for coaxial cylinders energized with power frequency or under negative DC polarization [14,34,41,42] can be expressed as:

$$E_{c,peak} = 31 m \delta (1 + 0.308/\sqrt{\delta r}) \quad (6)$$

According to He et al. [45], in a bundle conductor (6) also applies for each sub-conductor, r being the sub-conductor radius in cm.

For coaxial cylinders under positive DC polarization, the visual corona inception electric field in kV/cm is higher [46] and can be calculated as [41]:

$$E_{c,dc} = 33.7m\delta(1 + 0.241/\sqrt{\delta r}) \quad (7)$$

It is worth noting that according to Equations (5)–(7), the corona inception field strength depends on the radius of the conductor, its surface condition, the bundle spacing and atmospheric conditions as related to the relative air density.

Peek [47,48] also derived an empirical relationship for the corona inception field E_c of coaxial cylinders in air based on experimental data:

$$E_{c,peak}/\delta = 31.53 + 9.63/\sqrt{\delta r} \quad (8)$$

where $E_{c,peak}$ is in kV_{peak}/cm, r is the inner conductor radius in cm and δ is the relative air density. However, it is known that Equation (8) provides inaccurate results when $\delta r > 1$ cm. Zaengl et al. [49], based on the previous work of Peek, developed an improved analytical expression. Figure 1 shows both the measured values of $E_{c,peak}/\delta$ and the ones predicted by (8).

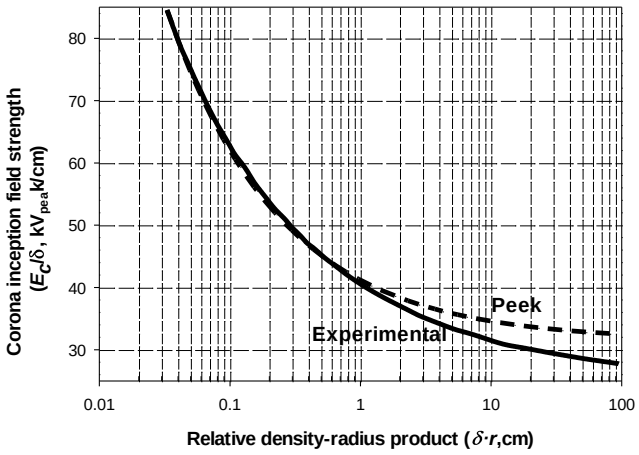

Figure 1. Corona inception field strength expressed as $E_{c,peak}/\delta$ for coaxial cylinders electrodes with air insulation. Adapted from [48].

Since it is easier to measure the voltage U (V) than the voltage gradient E (V/m), there are equations to determine E from experimental values of U, which are summarized in Figure 2. Both U and E can be expressed either in peak or root mean square (RMS) value.

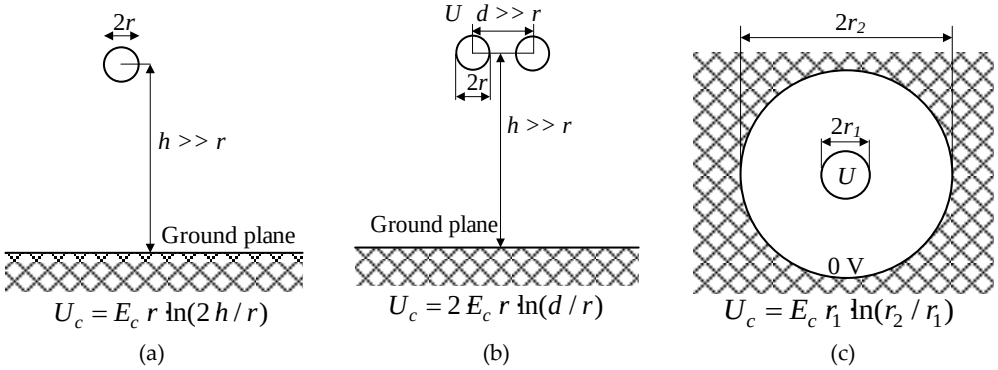

Figure 2. Relationship between the AC corona inception voltage U_c and the corona inception voltage gradient E_c [14,50]. (**a**) Single conductor; (**b**) Bifilar configuration; (**c**) Concentric cylinders.

When dealing with DC power lines, the space charge phenomena under different polarities cannot be ignored since it plays an important role in the breakdown process [51].

3. Environmental Conditions and Atmospheric Corrections

3.1. Environmental Conditions

Since low pressure increases the ionic and electronic mobility, this condition favors corona inception. Both the critical disruptive discharge voltage and the corona inception voltage tend to decrease when decreasing either air humidity and air density up to a point [36,52]. Maskell [53] found in coaxial cylindrical systems that the discharge current is reduced by about 20% when humidity varies from dry to saturation conditions at standard atmospheric conditions. However, when dealing with a relative humidity exceeding approximately 80%, this disruptive voltage can be irregular. It is believed that air humidity may affect the intensity of corona activity maybe because of the dirt accumulated on the conductor surface becomes rehydrated, thus resulting in more corona activity [54], although under fair weather conditions the effect of humidity in corona losses can be limited [50]. However, in Reference [55] it is pointed out that air humidity may influence some ionization parameters like electron attachment, and favors condensation which has measurable effects on the corona onset voltage gradient. In a study conducted by Garcia et al. [56] in Bogotá at an altitude of about 2540 m, it was concluded that when increasing the altitude above sea level, the influence of humidity in the breakdown voltage diminishes and the atmospheric correction factors proposed by the IEEE Std-4-1995 [57] to estimate the breakdown voltage may lead to significant errors.

Experiments conducted in bundle conductors at different pressures and air humidities indicate that the corona inception voltage decreases notably with the reduction of air pressure but this effect weakens with the increase of absolute air humidity when it is within 5–15 g/m^3, that is, when there is no condensation on the conductors' surface. However, when the absolute humidity is about 17.3 g/m^3, water drops due to condensation distort the surface electric field thus triggering a sudden drop of the corona inception voltage [58].

Therefore, environmental conditions have a strong influence on corona inception and breakdown values as recognized in different International Standards [36,59]. The greatest effect on corona generation occurs when transmission line conductors are contaminated and are wet due to foul weather conditions. There are other environmental conditions including damaging gases, vapors, conductive smoke from fires, fumes, excessive moisture, debris or extreme temperatures among others than can affect the performance of such devices [39].

Table 2 shows the standard atmosphere conditions as a function of the altitude above sea level from the ISO 2533:1975 standard [60], which is in close agreement with the values provided by [34] and [40].

Table 2. The standard atmosphere [60].

Altitude (m)	Temperature (°C)	Pressure (Pa)	Air Density (kg/m^3)	Relative Air Density, δ (-)
0	15.0	101,325.0	1.225000	1.000000
500	11.8	95,460.8	1.167270	0.952873
1000	8.5	89,874.6	1.111640	0.907463
1500	5.3	84,556.0	1.058070	0.863728
2000	2.0	79,495.2	1.006490	0.821625
2500	−1.3	74,682.5	0.956859	0.781109
3000	−4.5	70,108.5	0.909122	0.742140
3500	−7.8	65,764.1	0.863229	0.704677
4000	−11.0	61,640.2	0.819129	0.668677
4500	−14.3	57,728.3	0.776775	0.634102
5000	−17.5	54,019.9	0.736116	0.600911
5500	−20.8	50,506.8	0.697106	0.569066
6000	−24.0	47,181.0	0.659697	0.538528

3.2. Atmospheric Correction Factors

In this subsection the atmospheric correction factors recommended by the IEC 60060-1-2010 [61] and IEEE Std 4-2013 [36] for testing of equipment are described. They are based on the correction factor K [29]:

$$U = U_0 K = U_0(k_1 k_2) \tag{9}$$

where k_1 and k_2 being, respectively the air density and humidity correction factors, U the voltage at non-standard atmospheric conditions and U_0 the voltage at standard atmospheric conditions. It is worth noting that according to [36], Equation (9) is also valid for the disruptive discharge voltage, because it changes linearly with the atmospheric correction factor K.

The density correction factor k_1, which is accurate in the range $0.8 < k_1 < 1.05$ is calculated from:

$$k_1 = \left(\frac{p}{p_0} \cdot \frac{273 + t_0}{273 + t}\right)^m = \delta^m \tag{10}$$

where m is an exponent defined in Table 3. According to Equation (10), the dielectric strength of air gaps depends on δ^m. For long non-uniform gaps, in which the breakdown is dominated by both streamers and leaders, m < 1. Contrarily, for uniform air gaps shorter than 2 m, in which the breakdown is dominated by streamers, m = 1, since the strength of the air gap and the relative air density δ are almost proportional [3,4].

The humidity correction factor k_2 is calculated as:

$$k_2 = (k)^w \tag{11}$$

where w is an exponent defined in Table 3 and k is calculated depending on the test voltage type as:

$$\begin{cases} \text{dc}: \; k = 1 + 0.014(h_a/\delta - 11) - 0.00022(h_a/\delta - 11)^2 & 1 < h_a/\delta < \text{g/m}^3 \\ \text{ac}: \; k = 1 + 0.012(h_a/\delta - 11) & 1 < h_a/\delta < \text{g/m}^3 \\ \text{impulse}: \; k = 1 + 0.010(h_a/\delta - 11) & 1 < h_a/\delta < \text{g/m}^3 \end{cases} \tag{12}$$

where h_a is the absolute humidity in g/m^3.

Parameter g in Table 3, accounts for the type of pre-discharges, and is defined as:

$$g = U_{50}/(500 L \delta k) \tag{13}$$

where U_{50} is the 50% disruptive discharge voltage (kV$_{\text{peak}}$), that can either be estimated or measured at the real atmospheric conditions and L (m), the minimum discharge path. The value of L has a great influence on g and therefore on the correction factor K. When the U_{50} voltage is not available, it can be assumed as 1.1 times the test voltage.

Table 3. Parameters g, m and w [36,61].

g	m [1]	w [1,2]
<0.2	0.0	0.0
0.2–1.0	$g(g - 0.2)/0.8$	$g(g - 0.2)/0.8$
1.0–1.2	1.0	1.0
1.2–2.0	1.0	$(2.2 - g)(2.0 - g)/0.8$
>2.0	1.0	0.0

[1] Valid for altitudes below 2000 m; [2] w = 0 for operating voltages <72.5 kV or gap lengths <0.5 m.

4. Published Correction Factors

4.1. Sphere-Sphere Gap, Rod-Rod Gap and Rod-Plane Gaps

Sphere-sphere, rod-rod and rod-plane gaps are included in this review since they are commonly found in high-voltage laboratories, and often used as test or calibration gaps for many applications, some of which are related to transmission lines. The IEEE Std 4-2013 [36] provides tables of the disruptive voltage U_{d} of a sphere-sphere gap configuration for an average absolute humidity $h_a = 8.5\ \mathrm{g/m^3}$, and specifies that U_d increases linearly with the absolute humidity at a rate of $0.2\%/(\mathrm{g/m^3})$. Thus, for AC and impulse tests, this standard suggests applying a correction factor as:

$$U_d = U_0(k\delta) \tag{14}$$

where U_0 is the peak or impulse disruptive discharge voltage at the standard atmosphere and reference humidity $8.5\ \mathrm{g/m^3}$ and k is calculated as:

$$k = 1 + 0.002(h_a/\delta - 8.5) \tag{15}$$

where h_a is the ambient absolute humidity in $\mathrm{g/m^3}$.

Similarly, for the rod-rod gap configuration under DC stress, Reference [36] suggests applying the correction in (14) but U_0 is referenced to $11\ \mathrm{g/m^3}$, so factor k is now:

$$k = 1 + 0.014(h_a/\delta - 11) \tag{16}$$

Note that (16) is valid within the interval 1 and $13\ \mathrm{g/m^3}$.

Huang et al. [52] measured the corona inception voltage of a rod-plane gap geometry in a climate chamber using an ultraviolet camera. Results attained are summarized in Figure 3, which shows that the breakdown or critical disruptive voltage increase almost linearly with the pressure of air.

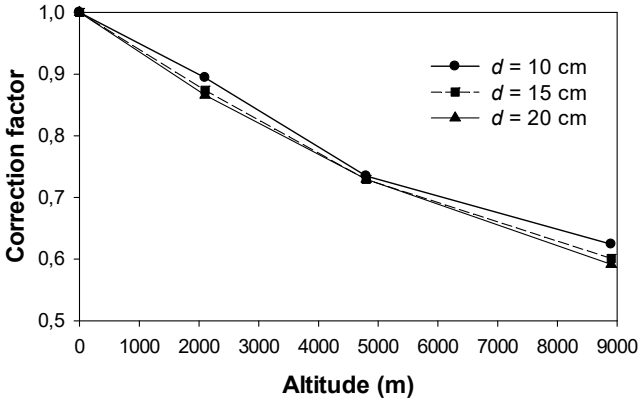

Figure 3. Rod-plane gap geometry adapted from Reference [52] by applying the hypsometric equation. Correction factor for the corona inception voltage as a function of the altitude for different gap lengths d at 25 °C and $16\ \mathrm{g/m^3}$.

4.2. Conductors of Circular Cross Section

According to results conducted in an artificial chamber by Hu et al. [58,62], the relationship between corona inception voltage $U_{c,RMS}$ and air pressure p for AC bundle conductors can be expressed as:

$$U_{c,RMS} = U_{c0,RMS}(p/p_0)^m \tag{17}$$

where $U_{c,RMS}$ and $U_{c0,RMS}$ are, respectively, the corona inception voltage in $\mathrm{kV_{RMS}}$ at a given air pressure p, and at standard air pressure p_0, and m an exponent within the range 0.59–0.91 depending on

the bundle configuration and the absolute air humidity [58]. Similarly, when there is no condensation on the conductors' surface, a suitable relationship between the corona inception voltage $U_{c,RMS}$ and air humidity h_a can be expressed as:

$$U_{c,RMS} = U_{c0,RMS}(h_a/h_{a,0})^n \tag{18}$$

where h_a and $h_{a,0}$ being, respectively, the measured absolute air humidity and the standard air humidity in g/m^3, and n an exponent within the range 0.038–0.190 depending on the bundle configuration and the pressure of air [58].

Tests conducted in a climate chamber varying the relative air density δ within the interval 0.55–0.95 using a smooth copper tube with outer diameter 19 mm suggested that the relation between corona inception voltage $U_{c,RMS}$ and δ for AC conductors can be expressed as [21]:

$$U_{c,RMS} = U_{c0,RMS}\delta^k \tag{19}$$

where $U_{c,RMS}$ and $U_{c0,RMS}$ are, respectively, the corona inception voltage in kV at a given relative air density δ and at unity air density, and k an exponent in the range 0.75–1. In Reference [21] it was also found that exponent k increases and thus the effect of δ on the corona inception voltage when decreasing the relative air humidity. According to [21], the combined effect of the relative air density δ and absolute humidity h_a can be expressed as:

$$U_{c,RMS} = U_{c0,RMS}\delta^{k'}(1 + h_a/\delta)^m \tag{20}$$

According to Phillips et al. [2], who carried out impulse voltage tests in 500 kV DC transmission lines and associated substation applications, the correction (19) must be applied with exponent k = 0.7–0.9 depending on the specific geometry:

$$U_{d,impulse} = U_{d0,impulse}\delta^k \tag{21}$$

where U_d and U_{d0} are, respectively, the critical disruptive voltages in kV at a given air relative density δ and at unity relative density.

Hu et al. [62] conducted power frequency corona inception voltage tests in a climatic chamber with cylindrical copper conductors of different diameters within a range of 16–25 mm, confirming that the relationship in Equation (19) is correct. They also found that exponent k depends on the absolute humidity, so $k \in (0.633, 0.771)$ when h_a is within 17.3–5 g/m^3. Note that exponent k is reduced when increasing the absolute humidity h_a, so that the impact on the corona inception voltage is less. Hu et al. [62] also indicated that Equation (20) can be applied when including the effect of absolute humidity. Analysis based on molecular gas dynamics [63] also corroborates that the DC voltage breakdown or flashover voltage satisfies Equation (19).

In DC systems, the corona inception voltage for positive polarity is lower than that for negative polarity, thus positive polarity determines the criterion to design transmission line insulation [64]. Bian et al. [65] conducted DC corona tests of both polarities of a four-conductor square bundle of conductors using an outdoor corona cage with defined ground planes under various atmospheric pressures. Two types of conductors were tested, with outer diameters 23.76 and 27.63 mm^2 and surface roughness factors m = 0.895 and 0.891, respectively. The authors found a linear decreasing relationship between the corona inception voltage U_c and the altitude h as follows:

$$\begin{cases} U_c{}^- = U_{c0}^-(1 - 0.0895h) \\ U_c{}^+ = U_{c0}^+(1 - 0.0915h) \end{cases} \tag{22}$$

where U_{c0} in kV is the corona inception voltage at sea level and h the altitude above sea level in km. Therefore, according to Equation (22), as the altitude increases by 1000 m, the negative corona inception

voltage decreases by 8.95% whereas the positive one decreases by 9.15%, so these trends are not in close agreement with Peek's formula [65].

Ortéga et al. [66] proposed a correction factor for the 50% breakdown voltage U_{50} of rod-plane air gaps subjected to positive-polarity lightning impulses based on laboratory tests, combining the effects of humidity and density:

$$U_{50} = U_{50}(\delta, h_a) - E[(\delta - 1) + 0.01(h_a - 11)]d \quad (23)$$

where U_{50} is the 50% breakdown voltage at standard atmospheric conditions, E = 500 kV/m and d (m) is the gap length.

Table 4 summarizes the most relevant correction factors detailed in this section.

Table 4. Summary of Correction Factors.

Author	Geometry	Correction Factor
Paschen [67]	Uniform field	$U_{d,peak} = \frac{B(pd)}{\ln(A)+\ln(pd)-\ln[\ln(1+1/\gamma)]}$
Peek [30–32,47]	Parallel. conductors, AC	$E_{c,peak} = 30m\delta(1 + 0.301/\sqrt{\delta r})$
Peek [32]	Coaxial cylinders, AC, DC−	$E_{c,peak} = 31m\delta(1 + 0.308/\sqrt{\delta r})$
Peek [32]	Coaxial cylinders, DC+	$E_{c,peak} = 33.7m\delta(1 + 0.241/\sqrt{\delta r})$
Peek [30–32]	Parallel conductors	$U_{d,peak} = E_{d,peak} rm\delta \ln(d/r)$
Westingh. [34]	Parallel conductors	$U_{d,p-to-n,RMS} = E_{d,RMS} rm\delta^{2/3} \ln(d/r)$
IEEE Std4 [36]	General	$U = U_0(k_1 \cdot k_2)$
IEEE Std4 [36]	Sphere-sphere gap, AC	$U_{d.peak} = U_{0,peak}(k\delta)k = 1 + 0.002(h_a/\delta - 8.5)$
IEEE Std4 [36]	Rod-rod gap, DC	$U_{d,dc} = U_{0,dc} \cdot (k\delta)k = 1 + 0.014(h_a/\delta - 11)$
Hu et al. [58]	Bundle conductors, AC	$U_{c,RMS} = U_{c0,RMS}(p/p_0)^m m \in (0.59, 0.91)$
Hu et al. [21]	Smooth conductors	$U_{c,RMS} = U_{c0,RMS}\delta^k$
Phillips et al. [2]	500 kV line; impulse	$U_{d,impulse} = U_{d0,impulse}\delta^k$
Hu et al. [62]	Cylindrical Conductors	$U_{c,RMS} = U_{c0,RMS}(p/p_0)^k k \in (0.633, 0.771)$
Bian et al. [65]	four-bundle conductors, DC	$\begin{cases} {U_{c,dc}}^- = U^-_{c0,dc}(1 - 0.0895h) \\ {U_{c,dc}}^+ = U^+_{c0,dc}(1 - 0.0915h) \end{cases}$
Ortéga et al. [66]	Rod-plane gap; +impulse	$U_{50} = U_{50}(\delta, h_a) - E[(\delta - 1) + 0.01(h_a - 11)]d$

E_c (U_c): corona inception voltage gradient (voltage) in kV/cm (kV); E_d (U_d): critical disruptive voltage gradient (voltage) in kV/cm (kV); δ: relative air density calculated from Reference [36]; r: conductor radius [m]; h: altitude above sea level [km]; p: pressure [Pa]; h_a: absolute humidity in g/m^3; E = 500 kV/m; d: gap length in m.

Figure 4 plots the voltage correction factors deduced from the summary presented in Table 4 as a function of the altitude above sea level taking into account the standard atmospheric conditions in Table 4.

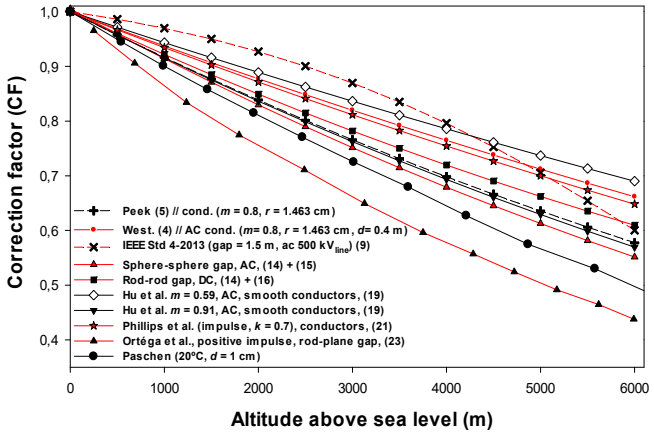

Figure 4. Altitude correction factors for critical disruptive and corona inception voltages according to the corrections summarized in Table 4 for r = 2.926/2 cm, m = 0.8, d = 40 cm, h_a = 11 g/m^3. Black lines are from equations based on corona inception conditions whereas red lines are from equations based on disruptive conditions.

Results from Figure 4 show clear differences between the different correction factors found in the technical literature, differences that tend to increase with the increasing altitude. From these results it is clear that the correction factor found in Ortéga et al. [66] sets a bottom limit.

It should be pointed out that some of the correction factors reviewed in this work come from research works (some of them derived from artificial simulation experiments), whereas others are found in International Standards. It is obvious that the correction factor to be applied depend on the specific geometry of the high-voltage electrodes considered and insulation structure.

Therefore, one can conclude that more research is required in order to gather as much data as possible of every specific high-voltage device and insulation structure to be installed in high-altitude regions, so that the pertinent International Standards and the knowledge of the high-voltage laboratories can be adapted to these new necessities.

The difficulty in measuring the electric field strength must be highlighted, although it is known that its value determines both corona onset and breakdown conditions, depending on the insulation structure. Therefore, most of the correction factors are obtained from the voltage applied but not from the electric field strength during corona onset or breakdown conditions, which is known to have a strong impact. This also requires further research, as well as a deep analysis of the feasibility and accuracy of applying combined experimental and numerical simulation methods to determine the electric field strength during such limit conditions, among other possible solutions.

4.3. Tabulated Altitude Correction Factors Found in International Standards

Since at high altitude, atmospheric air becomes less dense and a more effective thermal insulator, it is expected that electrical equipment using air as cooling and insulating medium (power line insulators and conductors, transformer bushings, switches, dampers or switchgear support insulators among others) will experience a higher temperature rise and will have a lower dielectric strength when operated at higher altitudes compared to when operating at altitudes below 1000 m [39]. Consequently, voltage and current derating are often applied. Figure 5 shows the tabulated altitude correction factors according to the ANSI C37.30 [39] standard for high-voltage air switches, insulators, and bus supports and the dielectric strength correction factors for altitudes greater than 1000 m suggested by the IEEE C57.13 standard [38] for instrument transformers. Figure 5 also includes the correction factors for insulation distances proposed by the ANSI/EIA 364-20D standard [68] related to electrical connectors, sockets, and coaxial contacts, which take into account the effect of pressure when such devices operate at high altitude.

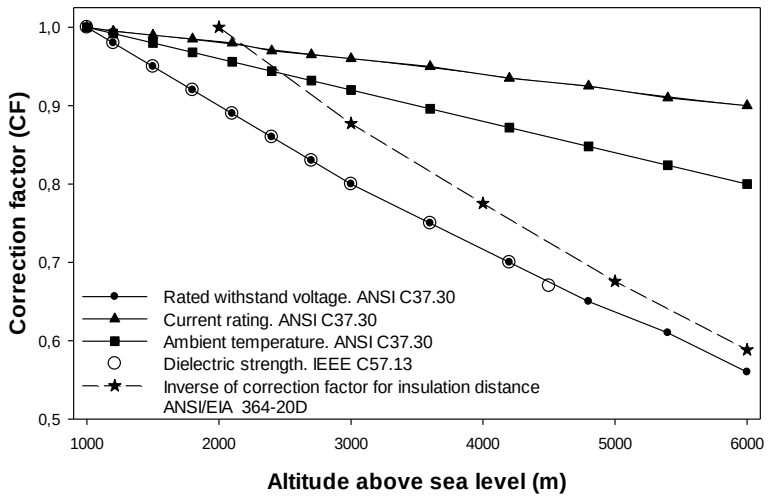

Figure 5. Altitude correction factors according to the ANSI C37.30 standard [39], dielectric strength correction factor according to the IEEE C57.13 standard [38] and correction factors for insulation distances proposed by the ANSI/EIA 364-20D standard [68].

It is noted that although different types of power frequency electric field sensors are commercially available, such as optical, capacitive or field mills [69,70], a direct measurement of the electric field strength to determine the corona onset or breakdown conditions is still a challenging problem. Such electric field sensors are either complex, have movable parts, are intrusive, present limited sensitivity or are expensive [71], so a universal solution does not exist.

5. Conclusions

This paper has presented a comprehensive literature review of the available atmospheric correction factors to limit corona activity and ensuring proper performance when planning air-insulated transmission lines intended for high-altitude areas. This topic is generating a growing interest due to the recent construction and the projects of EHV and UHV transmission lines and the associated substations crossing high-altitude regions. Some of the correction factors reviewed in this paper were obtained from real or artificial experiments found in different research works, whereas others come from different standards. Altitude correction factors found in the technical literature and results from the latest research show important differences among them, which tend to increase with the altitude. It is suggested to conduct more research and to gather more data of every specific high-voltage device to be installed in high-altitude regions, in order to adapt and update the pertinent International Standards to the new findings, and the knowledge of the high-voltage laboratories to these new necessities. This fact is important since the correction factors to be applied are highly dependent on the geometry of the high-voltage component under analysis. The authors' hope is that more studies outside the range of altitude from which most prior research has been based, will increase.

This paper has also highlighted the difficulty of measuring the electric field strength, which is known to determine both corona onset and breakdown conditions, depending on the insulation structure. Due to this fact, most of the correction factors are obtained from the voltage applied but not from the electric field strength during corona onset or breakdown conditions and, therefore, this topic also requires further research.

Author Contributions: J.-R.R. designed and performed most of the bibliographic review, W.L. reviewed all data and equations, and J.R. guided and supervised the atmospheric and altitude correction factors.

Funding: This research received no external funding.

Conflicts of Interest: The authors declare no conflicts of interest.

References

1. Nelson, J.P. High-Altitude Considerations for Electrical Power Systems and Components. *IEEE Trans. Ind. Appl.* **1984**, *IA-20*, 407–412. [CrossRef]
2. Phillips, T.; Robertson, L.; Rohlfs, A.; Thompson, R. Influence of Air Density on Electrical Strength of Transmission Line Insulation. *IEEE Trans. Power Appar. Syst.* **1967**, *PAS-86*, 948–961. [CrossRef]
3. Rickmann, J.; Elg, A.-P.; Fan, J.; Li, Q.; Liao, Y.; Pigini, A.; Tabakovic, D.; Wu, D.; Yujian, D. Current State of Analysis and Comparison of Atmospheric and Altitude Correction Methods for Air Gaps and Clean Insulators. In Proceedings of the 19th International Symposium on High Voltage Engineering, Pilsen, Czech Republic, 23–28 August 2015; pp. 1–6.
4. Wu, D.; Li, M.; Kvarngren, M. Uncertainties in the application of atmospheric and altitude corrections as recommended in IEC standards. In Proceedings of the 16th International Symposium on High Voltage Engineering, Cape Town, South Africa, 24–28 August 2009; pp. 1–6.
5. Du, Z.; Huang, D.; Qiu, Z.; Shu, S.; Ruan, J.; Huang, D.; Shu, S.; Du, Z. Prediction study on positive DC corona onset voltage of rod-plane air gaps and its application to the design of valve hall fittings. *IET Gener. Transm. Distrib.* **2016**, *10*, 1519–1526. [CrossRef]
6. Qi-fa, W.; Wei-ning, W.; Yong, C. Discussion of UHV transmission line insulation design and the effect on environment. In Proceedings of the Intrrnational Workshop on UHVAC Transmission Technology, Beijing, China, 2005; pp. 46–57.

7. Erich Heberlein, G.; Malkowski, C.; Cibulka, M.J. The effect of altitude on the operation performance of low voltage switchgear and controlgear components. In *Conference Record of the 2000 IEEE Industry Applications Conference. Thirty-Fifth IAS Annual Meeting and World Conference on Industrial Applications of Electrical Energy (Cat. No.00CH37129)*; IEEE: Piscataway, NJ, USA, 2000; Volume 4, pp. 2688–2694.
8. Hu, J.; Sun, C.; Jiang, X.; Yang, Q.; Zhang, Z.; Shu, L. Model for Predicting DC Flashover Voltage of Pre-Contaminated and Ice-Covered Long Insulator Strings under Low Air Pressure. *Energies* **2011**, *4*, 628–643. [CrossRef]
9. Pedersen, A. Calculation of Spark Breakdown or Corona Starting Voltages in Nonuniform Fields. *IEEE Trans. Power Appar. Syst.* **1967**, *PAS-86*, 200–206. [CrossRef]
10. Pedersen, A. On the electrical breakdown of gaseous dielectrics-an engineering approach. *IEEE Trans. Electr. Insul.* **1989**, *24*, 721–739. [CrossRef]
11. Riba, J.-R.; Abomailek, C.; Casals-Torrens, P.; Capelli, F. Simplification and cost reduction of visual corona tests. *IET Gener. Transm. Distrib.* **2018**, *12*, 834–841. [CrossRef]
12. Lucas, J.R. *High Voltage Engineering*; University of Moratuwa: Moratuwa, Sri Lanka, 2001; p. 204.
13. Schlabbach, J.; Rofalski, K.H. *Power System Engineering: Planning, Design, and Operation of Power Systems and Equipment*; WILEY-VCH Verlag GmbH & Co.: Weinheim, Germany, 2008; ISBN 978-3-527-40759-0.
14. Electric Power Research Institute. *Transmission Line Reference Book 345 kV and above*, 2014th ed.; Electric Power Research Institute (EPRI): Palo Alto, CA, USA, 2014.
15. USDA. *Design Manual for High Voltage Transmission Lines*; USDA: Washington, DC, USA, 2005.
16. Hernández-Guiteras, J.; Riba, J.-R.; Casals-Torrens, P. Determination of the corona inception voltage in an extra high voltage substation connector. *IEEE Trans. Dielectr. Electr. Insul.* **2013**, *20*, 82–88. [CrossRef]
17. Huang, S.; Liu, Y.; Chen, S.; Zhou, G.; Zhuang, W. Corona Onset Characteristics of Bundle Conductors in UHV AC Power Lines at 2200 m Altitude. *Energies* **2018**, *11*, 1047. [CrossRef]
18. Robertson, L.M.; Wagner, C.F.; Bliss, T.J. Colorado High-Altitude Corona Tests I—Scope, Tests, and Instrumentation. *Trans. Am. Inst. Electr. Eng. Part III Power Appar. Syst.* **1957**, *76*, 356–364. [CrossRef]
19. Robertson, L.M.; Lantz, A.D. Colorado High-Altitude Corona Tests II—Insulators and Associated Hardware. *Trans. Am. Inst. Electr. Eng. Part III Power Appar. Syst.* **1957**, *76*, 366–369. [CrossRef]
20. Robertson, L.M.; Shankle, D.F.; Smith, J.C.; O'neil, J.E. Leadville High-Altitude Extra-High-Voltage Test Project Part II—Corona-Loss Investigations. *Trans. Am. Inst. Electr. Eng. Part III Power Appar. Syst.* **1961**, *80*, 725–732. [CrossRef]
21. Hu, Q.; Shu, L.; Jiang, X.; Zhang, Z.; Hu, J. Effect of Atmospheric Parameters on AC Corona Onset Voltage of Conductors. In Proceedings of the 2010 International Conference on High Voltage Engineering and Application, New Orleans, LA, USA, 11–14 October 2010; pp. 417–420.
22. Yu, Q.; Ji, Y.; Zhang, Z.; Wen, Z.; Feng, C. Design and research of high voltage transmission lines on the Qinghai–Tibet Plateau—A Special Issue on the Permafrost Power Lines. *Cold Reg. Sci. Technol.* **2016**, *121*, 179–186. [CrossRef]
23. Xie, L.; Zhao, L.; Lu, J.; Cui, X.; Ju, Y. Altitude Correction of Radio Interference of HVDC Transmission Lines Part I: Converting Method of Measured Data. *IEEE Trans. Electromagn. Compat.* **2017**, *59*, 275–283. [CrossRef]
24. Zhao, L.; Cui, X.; Xie, L.; Lu, J.; He, K.; Ju, Y. Altitude Correction of Radio Interference of HVdc Transmission Lines Part II: Measured Data Analysis and Altitude Correction. *IEEE Trans. Electromagn. Compat.* **2017**, *59*, 284–292. [CrossRef]
25. He, W.; Wan, B.; Lan, L.; Pei, C.; Zhang, J.; Chen, Y.; Chen, X.; Wen, X. Effect of Altitude on the Audible Noise Level of AC Power lines. *Energies* **2017**, *10*, 1055. [CrossRef]
26. Biswas, H.; Sharma, V.D.; Chibber, O.P.; Ray, S.K. Himalayas Challenge 400-kV Installation. *Transm. Distrib. World Mag.* **2008**, *60*, 44–51.
27. Cross Border Indo-Nepal Transmission Line project. Available online: http://sjvn.nic.in/writereaddata/Portal/Images/transmission_line_18_04_13.pdf (accessed on 11 December 2017).
28. Línea de Transmisión de 500 kV Mantaro-Marcona-Socabaya-Montalvo (917 km). Available online: https://www.osinergmin.gob.pe/seccion/centro_documental/electricidad/Documentos/PROYECTOSGFE/Acordeón/Transmisión/2.1.1.pdf (accessed on 11 December 2017).
29. Gutman, I.; Pigini, A.; Rickmann, J.; Fan, J.; Wu, D.; Gockenbach, E. Atmospheric and altitude correction of air gaps, clean and polluted insulators: State-of-the-art within CIGRÉ and IEC. In *CIGRÉ Session 2014*; Cigré: Paris, France, 2014; pp. 1–10.

30. Peek, F.W. The Law of Corona and the Dielectric Strength of Air-II. *Proc. Am. Inst. Electr. Eng.* **1911**, *30*, 1051–1092. [CrossRef]
31. Peek, F.W. Law of Corona and Dielectric Strength of Air-III. *Trans. Am. Inst. Electr. Eng.* **1913**, *XXXII*, 1767–1785. [CrossRef]
32. Peek, F.W. The Law of Corona and the Dielectric Strength of Air-IV The Mechanism of Corona Formation and Loss. *Trans. Am. Inst. Electr. Eng.* **1927**, *XLVI*, 1009–1024. [CrossRef]
33. Krasniqi, I.; Komoni, V.; Alidemaj, A.; Kabashi, G. Corona losses dependence from the conductor diameter. In Proceedings of the 10th WSEAS international conference on System science and simulation in engineering, Penang, Malaysia, 3–5 October 2011.
34. *The Central Station Engineers of the Westinghouse Eectric Corporation, Electrical Transmission and Distribution Reference Book*; Westinghouse: East Pittsburgh, PA, USA, 1964.
35. Li, Z.-X.; Fan, J.-B.; Yin, Y.; Chen, G. Numerical calculation of the negative onset corona voltage of high-voltage direct current bare overhead transmission conductors. *IET Gener. Transm. Distrib.* **2010**, *4*, 1009–1015. [CrossRef]
36. IEEE. *4-2013—IEEE Standard for High-Voltage Testing Techniques*; IEEE: Piscataway, NJ, USA, 2013. [CrossRef]
37. IEEE. *C37.04-1999—IEEE Standard Rating Structure for AC High-Voltage Circuit Breakers*; IEEE: Piscataway, NJ, USA, 1999. [CrossRef]
38. IEEE. *C57.13-2016—IEEE Standard Requirements for Instrument Transformers*; IEEE: Piscataway, NJ, USA, 2008; ISBN 978-0-7381-5411-4.
39. IEEE. *ANSI/IEEE C37.30-1971—American National Standard Definitions and Requirements for High-Voltage Air Switches, Insulators, and Bus Supports*; IEEE: Piscataway, NJ, USA, 1971. [CrossRef]
40. Institute, E.P.R. *EPRI AC Transmission Line Reference Book: 200 kV and Above*, 2014th ed.; Electric Power Research Institute: Palo Alto, CA, USA, 2014.
41. Addendum to Doc.20: Interferences Produced by Corona Effect of Electric Systems. Available online: https://e-cigre.org/publication/061-addendum-to-doc20--interferences-produced-by-corona-effect-of-electric-systems (accessed on 10 July 2018).
42. Naidu, M.S.; Kamaraju, V. *High Voltage Engineering*; Tata McGraw-Hill Publishing Company Limited: New York, NY, USA, 1996; ISBN 0-07-462286-2.
43. Carsimamovic, A.; Mujezinovic, A.; Carsimamovic, S.; Bajramovic, Z.; Kosarac, M.; Stankovic, K. Calculation of the corona onset voltage gradient under variable atmospheric correction factors. In Proceedings of the IEEE EUROCON 2015—International Conference on Computer as a Tool (EUROCON), Salamanca, Spain, 8–11 September 2015; pp. 1–5.
44. Fridman, A.; Fridman, A.; Kennedy, L.A. *Plasma Physics and Engineering*, 2nd ed.; CRC Press: Boca Raton, FL, USA, 2011; ISBN 9781439812280.
45. He, W.; He, J.; Wan, B.; Chen, Y.; Pei, C.; Chen, Y. Influence of altitude on radio interference level of AC power lines based on corona cage. *IET Sci. Meas. Technol.* **2015**, *9*, 861–865. [CrossRef]
46. Zheng, Y.; Zhang, B.; He, J. Current-voltage characteristics of dc corona discharges in air between coaxial cylinders. *Phys. Plasmas* **2015**, *22*, 023501. [CrossRef]
47. Peek, F.W. *Dielectric phenomena in high-voltage engineering*; McGraw-Hill Book Company, Inc.: New York, NY, USA, 1929.
48. Kuffel, J.; Zaengl, W.S.; Kuffel, P. *High Voltage Engineering Fundamentals*, 2nd ed.; Elsevier: New York City, NY, USA, 2000; ISBN 978-0-7506-3634-6.
49. Zaengl, W.S.; Nyffenegger, H.U. Critical Field Strength for Cylindrical Conductors in Air: An Extension of Peek's Formula. In Proceedings of the 3rd International Conference on Gas Discharges, London, UK, 9–12 September 1974; pp. 302–305.
50. Yin, F.; Farzaneh, M.; Jiang, X. Corona investigation of an energized conductor under various weather conditions. *IEEE Trans. Dielectr. Electr. Insul.* **2017**, *24*, 462–470. [CrossRef]
51. Al-Hamouz, Z.M. Corona power loss, electric field, and current density profiles in bundled horizontal and vertical bipolar conductors. *IEEE Trans. Ind. Appl.* **2002**, *38*, 1182–1189. [CrossRef]
52. Huang, W.; He, Z.; Cai, W.; Deng, H.; Deng, W.; Qin, H. Study on the environmental factors of rod-plane gap discharge based on UV imaging. *Gaodianya Jishu/High Volt. Eng.* **2015**, *41*, 2788–2794. [CrossRef]

53. Maskell, B.R. The Effect of Humidity on a Corona Discharge in Air. Available online: https://www.researchgate.net/publication/235121402_The_Effect_of_Humidity_on_a_Corona_Discharge_in_AiR (accessed on 10 July 2018).
54. Pretorius, P.H.; Britten, A.C.; Govender, T.; Hubbard, K.R.; Mahatho, N.; Parus, N. On the electromagnetic interference associated with the power line carrier system of the cahora bassa hvdc line—A hypothesis based on recent investigations and observations. In *Cigré Session 2012*; Cigré: Paris, France, 2012; pp. 1–8.
55. Maruvada, P.S.; Bisnath, S. *Corona in Transmission Systems: Theory, Design and Performance*; Crown Publications: Johannesburg, South Africa, 2011; ISBN 9780620493888.
56. Garcia, J.; Herrera, F.; Ortiz, H. Study of the breakdown voltage of the air in high altitudes, applying lightning impulses (1.2/50 s) under conditions of controlled humidity and temperature. In Proceedings of the 1999 Eleventh International Symposium on High Voltage Engineering, London, UK, 27–23 August 1999.
57. IEEE. *4-1995—IEEE Standard Techniques for High-Voltage Testing*; IEEE: Piscataway, NJ, USA, 1995. [CrossRef]
58. Hu, Q.; Shu, L.; Jiang, X.; Sun, C.; Zhang, S.; Shang, Y. Effects of air pressure and humidity on the corona onset voltage of bundle conductors. *IET Gener. Transm. Distrib.* **2011**, *5*, 621–629. [CrossRef]
59. IEEE. *IEEE Standard Definitions of Terms Relating to Corona and Field Effects of Overhead Power Lines*; IEEE: Piscataway, NJ, USA, 2005. [CrossRef]
60. ISO ISO 2533:1975—Standard Atmosphere. Available online: https://www.iso.org/standard/7472.html (accessed on 10 July 2018).
61. High-voltage test techniques—Part 1: General definitions and test requirements. Available online: https://webstore.iec.ch/publication/300 (accessed on 10 July 2018).
62. Hu, Q.; Shu, L.; Jiang, X.; Sun, C.; Yuan, Q.; Yang, Z. Effect of Atmospheric Factors on AC Corona Inception Voltage of Conductors and Its Correction. *Power Syst. Technol.* **2010**, *34*, 70–76.
63. Liu, D.-M.; Guo, F.-S.; Sima, W.-X. Modification of DC Flashover Voltage at High Altitude on the Basis of Molecular Gas Dynamic. *J. Electr. Eng. Technol.* **2015**, *10*, 625–633. [CrossRef]
64. Chan, J.K.; Kuffel, J.; Sibilant, G.C.; Bell, J. Methodology for HVDC corona tests. In *2016 CIGRE-IEC Colloquium*; Cigré: Montréal, QC, Canada, 2016; pp. 1–10.
65. Bian, X.; Wang, L.; Liu, Y.; Yang, Y.; Guan, Z. High Altitude Effect on Corona Inception Voltages of DC Power Transmission Conductors Based on the Mobile Corona Cage. *IEEE Trans. Power Deliv.* **2013**, *28*, 1971–1973. [CrossRef]
66. Ortéga, P.; Waters, R.T.; Haddad, A.; Hameed, R.; Davies, A.J. Impulse breakdown voltages of air gaps: A new approach to atmospheric correction factors applicable to international standards. *IEEE Trans. Dielectr. Electr. Insul.* **2007**, *14*, 1498–1508. [CrossRef]
67. Dakin, T.W.; Luxa, G.; Oppermann, G.; Vigreux, J.; Wind, G.; Winkelnkemper, H. Breakdown of gases in uniform fields—Paschen's curves for air, N2 and SF6. *Elektra* **1974**, *32*, 61–82.
68. Electronic components industry association. *Withstanding Voltage Test Procedure for Electrical Connectors, Sockets and Coaxial Contacts: EIA-364-20E*; Electronic Components Industry Association (ECIA): Englewood, CO, USA, 2015.
69. Xiao, D.; Ma, Q.; Xie, Y.; Zheng, Q.; Zhang, Z. A Power-Frequency Electric Field Sensor for Portable Measurement. *Sensors* **2018**, *18*, 1053. [CrossRef] [PubMed]
70. Yazdani, M.; Thomson, D.J.; Kordi, B. Passive Wireless Sensor for Measuring AC Electric Field in the Vicinity of High-Voltage Apparatus. *IEEE Trans. Ind. Electron.* **2016**, *63*, 4432–4441. [CrossRef]
71. Mahomed, F. Circuit Level Modelling of a Capacitive Electric Field Sensor. Mater Thesis, University of Witwatersrand, Johannesburg, South Africa, 2012.